

Impedance Modeling In Low Emittance Ring

ICFA Mini-Workshop on Impedances and Beam Instabilities in Particle Accelerators

A. Blednykh
Benevento, September 19-22, 2017



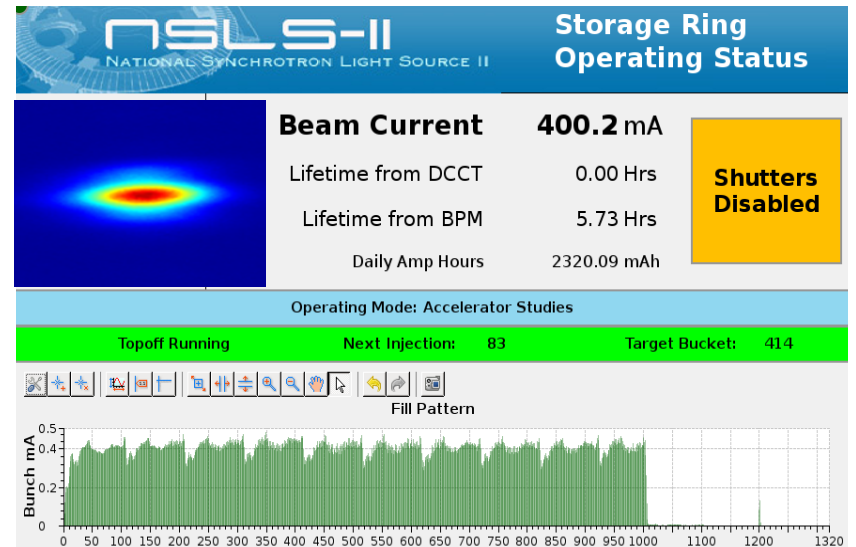
Outlook

- Intensity Increasing in NSLS-II
- Impedance modeling & Impedance Budget for $\sigma_s = 0.3\text{mm}$
- Microwave Instability Measurements in NSLS-II
- Beam Dynamics Simulations with $W_{||,\text{tot}}(s)$
- Concluding Remarks

NSLS-II Beam Intensity Increasing

02 Jul. 2014	25 mA with CESR-B SC RF cavity
11 Jul. 2014	First time at 50mA
14 Jul. 2014	Shutdown for ID and FE installation
03 Oct. 2104	Start of ID commissioning
23 Oct. 2014	First light on beamline flag!
11 Feb. 2015	Beamline operations begins at 25 mA
25 Feb. 2015	50 mA with IVU's magnet gap closed
11 Mar. 2015	First time at 100 mA
15 Apr. 2015	First time at 150 mA
17 Apr. 2015	Beamline operations begins at 50 mA
23 Apr. 2015	First time at 200 mA
Jul. 2015	Beamline operations begins at 150 mA
28 Jul. 2015	First time at 300 mA
Oct. 2015	Start operation with Top Off at 150 mA
04 Jan. 2016	Start operation with 2 nd RF cavity
29 Jan. 2016	Beamline operations begins at 175 mA

16 Feb. 2016	First time at 350 mA
17 Feb. 2016	Beamline operations begins at 200 mA
14 Apr. 2016	Beamline operations begins at 250 mA
18 Apr. 2016	First time at 400 mA
16 Feb. 2017	Beamline operations begins at 275 mA
05 Apr. 2017	Beamline operations begins at 300 mA
20 Jul. 2017	Beamline operations begins at 325 mA



NSLS-II Parameters

Energy,	3
Revolution period,	2.6
Momentum compaction,	3.7×10^{-4}
Energy loss,	287 (BM) 674 (BM + 3DW's)
RF voltage,	3.4
Synchrotron tune,	9.2×10^{-3} (BM + 3DW's)
Damping time,	54, 27 (w/o DWs) 23, 11.5 (with 3DWs)
Energy spread,	5×10^{-4} (BM) 8.7×10^{-4} (BM + 3DW's)
Bunch duration,	2.5 (w/o DWs) 4.3 (with 3DWs) Ignoring bunch lengthening

- Two 500MHz SC RF cavities presently installed in NSLS-II

Software and Analytical Approach

- Several 2D & 3D electrodynamics codes available for time domain and frequency domain numerical simulations, *GdfidL*, *CST*, *HFSS*, *ECHO*, *URMEL*, *Vorpal*, *ACE3P*, *ABCI*, *Poisson/Superfish*,
- The code choice for the time domain simulations: parallel computing, complexity of the geometries and bunch length considered for calculations, cross-checking with analytical results at least for simplified geometries.
- Impedance model, longitudinal and transverse, needs to be calculated for a bunch length much shorter than the length of the circulated bunch, stabilizing effect of positive chromaticity and microwave instability thresholds analysis.
- Simulations of 3D geometries for short bunch length will require to increase the computer power resources (mesh size decreasing) or to have the code with dispersion free algorithms, window moving mesh algorithm or standard algorithm.
- Most of 3D electrodynamics codes are commercial.
- Analytical Approach – for simplified geometries.

Computer Cluster Resources

First NSLS-II Accelerator Physics Cluster Generation



Supported by:

2007

S. Ozaki
S. Krinsky

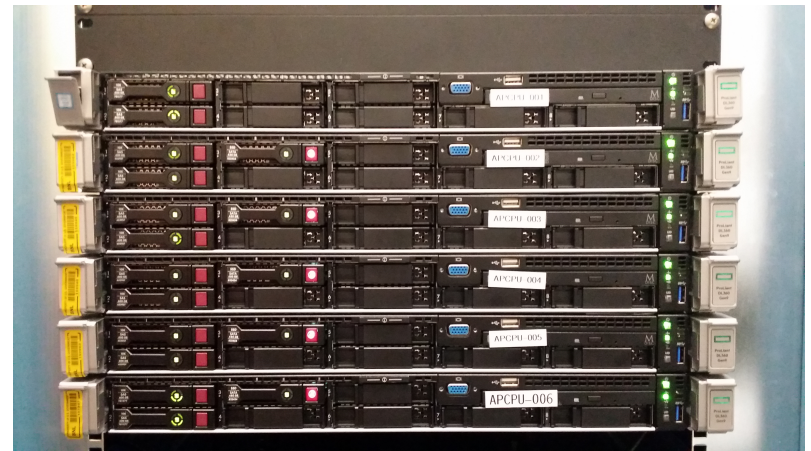
2009

F. Willeke
S. Krinsky

- Upgraded from Sep. 2006 to 2011
- **336 Cores & 1334GB Total Memory (RAM)**

- Computer cluster is necessary for numerical simulations of the Impedance Budget
- 3D electrodynamics parallel computing codes require significant computer resources for simulations with bunch length, $\sigma_z \ll 3mm$

Second NSLS-II Accelerator Physics Cluster Generation



Supported by: T. Shaftan / V. Smaluk (2016)

- Intel(R) Xeon(R) CPU E5-2699 v4 @ 2.20GHz
- **264 Cores & 3102GB Total Memory (RAM)**

```
Wall Clock Time: 3700 Seconds, diff: 75, GFlop/s: 37.36
The used connection Bandwidth is 22.70 MByte/s/Worker in 42 Messages/s/Worker.
*****
Timestep 5000 has been performed. The simulated Time is 254.4148e-12 Seconds.
The Wakepotentials are known up to s= 63.7936e-3 Metres.
CPU Time : 449983 Seconds, diff: 8916, MFlop/s: 313.49
Wall Clock Time: 3775 Seconds, diff: 75, GFlop/s: 37.37
The used connection Bandwidth is 22.70 MByte/s/Worker in 42 Messages/s/Worker.
```

Impedance Modeling Diagram

Excel

Vacuum Apertures
Lattice

Mathematica

3D GdfidL

2D ECHO

Analytical

Software for $W(s)$ &
 $Z(w)$ Simulations

MatLab

Results Crosschecking,
Numerical vs Analytical

Impedance Budget

Data Post-Processing
& Preparation

SPACE

ELEGANT

Vlasov-Fokker-Planck (VFP)
Particle Tracking Simulations

Analytical

Instability Thresholds
& Collective Effects

W. Bruns, <http://www.gdfidl.de>

I. Zagorodnov and T. Weiland, *Phys. Rev. ST Accel. Beams* 8, 042001 (2005)

I. Zagorodnov, *Phys. Rev. ST Accel. Beams* 9, 102002 (2006).

M. Borland, "elegant: A Flexible SDDS-Compliant Code for Accelerator Simulation," Argonne National Laboratory, ANL/APS/LS-287, 2000

G. Bassi, A. Blednykh, and V. Smaluk, *Phys. Rev. Accel. Beams*, vol. 19, p. 024401, 2016

Impedance/Vacuum Apertures Lattice

Imped_Lattice_Is_June8_2017

Cells: 6, 14, 20 and 26

From left to right	S(mm)	betax(m)	betay(m)	L(mm)	L(mm)*4	RW	Conductivity	Radius (ry), m	s0	k
Fast Corrector	48533.65	21.35395438	8.764469694	168.5	674	Inc	775194	0.0125	0.00010226	
BLW5(SS)	48702.15	21.28513577	8.346447559	5.540	22.16	SS	1350000	0.0125	8.49962E-05	
BLW5(GCu)	48707.69	21.28292024	8.332989857	52.310	209.24	Cu	54050000	0.0127	2.51097E-05	
BLW5(Ag)	48760	21.26214855	8.206817181	69.170	276.68	Ag	63000000	0.0125	2.36082E-05	
CHM1	48829.17	21.23509252	8.042471831	3956.3	15825.2	Al	31600000	0.0125	2.97131E-05	
BLW6(SS)	52785.47	20.46575214	3.369298068	5.540	22.16	SS	1350000	0.0125	8.49962E-05	
BLW6(GCu)	52791.01	20.46574729	3.369288602	77.710	310.84	Cu	54050000	0.0127	2.51097E-05	
BLW6(Ag)	52868.72	20.46599535	3.370775402	69.170	276.68	Ag	63000000	0.0125	2.36082E-05	
CHM2	52937.89	20.46671258	3.375132019	3956.2	15824.8	Al	31600000	0.0125	2.97131E-05	
BLW5(SS)	56894.09	21.28587228	8.350921296	5.540	22.16	SS	1350000	0.0125	8.49962E-05	
BLW5(GCu)	56899.63	21.28809181	8.364403268	52.310	209.24	Cu	54050000	0.0127	2.51097E-05	
BLW5(Ag)	56951.94	21.30919695	8.492601424	69.170	276.68	Ag	63000000	0.0125	2.36082E-05	
Fast Corrector	57021.11	21.33751506	8.664612992	168.5	674	Inc	775194	0.0125	0.00010226	
				8655.96	34623.84					

Cell 2 - EPU Straight Section

From left to right	S(mm)	betax(m)	betay(m)	L(mm)		RW	Conductivity	Radius (ry), m	s0	k
Fast Corrector				168.5		Inc	775194	0.0125	0.00010226	
BLW6(SS)				5.540		SS	1350000	0.0125	8.49962E-05	
BLW6(GCu)				77.710		Cu	54050000	0.0127	2.51097E-05	
BLW6(Ag)				69.170		Ag	63000000	0.0125	2.36082E-05	
CHM1				891.000		SS	1350000	0.0125	8.49962E-05	
TPR1				200		Cu	54050000	0.009125	2.01431E-05	
EPUCHM1				4844.800		NEG	2.00E+06	0.00575	4.44296E-05	
TPR2				315.000		Cu	54050000	0.009125	2.01431E-05	
BLW5(SS)				5.540		SS	1350000	0.0125	8.49962E-05	
BLW5(GCu)				52.310		Cu	54050000	0.0127	2.51097E-05	
BLW5(Ag)				69.170		Ag	63000000	0.0125	2.36082E-05	
CHM2				1636.300		Al	31600000	0.0125	2.97131E-05	
FlangeABS1				25.400		Cu	54050000	0.0115	2.35019E-05	
BLW5(SS)				5.540		SS	1350000	0.0125	8.49962E-05	
BLW5(GCu)				52.310		Cu	54050000	0.0127	2.51097E-05	
BLW5(Ag)				69.170		Ag	63000000	0.0125	2.36082E-05	
Fast Corrector				168.5		Inc	775194	0.0125	0.00010226	
				8655.96						

Cell 4 - IVU Straight Section

From left to right	S(mm)	betax(m)	betay(m)	L(mm)		RW	Conductivity	Radius (ry), m	s0	k
Fast Corrector				168.500		Inc	775194	0.012500	0.000102260	
BPMCHM				227.800		SS	1350000	0.012500	0.000084996	
RI W5(SS)				5.540		SS	1350000	0.012500	0.000084996	

Microsoft Excel Spreadsheet

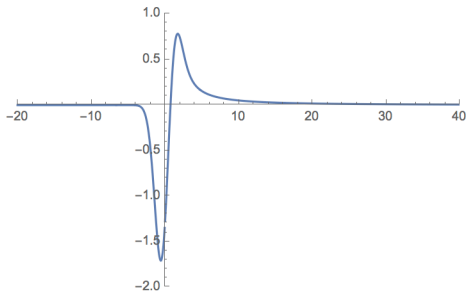
- At the beginning of the project the vacuum apertures lattice is unknown.
- Impedance analysis begins for a preliminary geometry some of the components.
- It can take several iterations on impedance optimization until the design will be finalized.
- Communication with RF, Diagnostic, Vacuum, Engineering, Mechanical groups is very important.
- Microsoft Excel is used to keep track on changes in the vacuum apertures lattice.
- As the final, the apertures in the arcs of the storage ring are fixed, but in the straight sections they will be updated based on ID's installation.
- Vacuum apertures lattice should be flexible and convenient for changes.
- Conductivity, radius and length from the Microsoft Excel Spreadsheet are used as the input parameters for the rw wakefield simulations in Mathematica script.

Resistive Wall Wakefield Simulations

Wrw_06142026

```
fbessel[u_] :=
If[u < 0,
Abs[u]3/2 e-u2/4
(BesseLI[1/4, u2/4] - BesseLI[-3/4, u2/4] - BesseLI[-1/4, u2/4] + BesseLI[3/4, u2/4]),
Abs[u]3/2 e-u2/4
(BesseLI[1/4, u2/4] - BesseLI[-3/4, u2/4] + BesseLI[-1/4, u2/4] - BesseLI[3/4, u2/4])]
```

```
Plot[fbessel[x], {x, -20, 62.5}, PlotRange -> {{-20, 40}, {-2, 1}}]
```



```
bCu = {0.0125, 0.0125, 0.0127, 0.0125, 0.0125, 0.0125, 0.0127, 0.0125, 0.0125, 0.0125,
0.0127, 0.0125, 0.0125};
Z0 = 120 * 3.1415;
con = {775 194, 1 350 000, 54 050 000, 63 000 000, 31 600 000, 1 350 000, 54 050 000, 63 000 000,
31 600 000, 1 350 000, 54 050 000, 63 000 000, 775 194};
oz = 0.3 * 10-3;
Lrw = {168.5, 5.540, 52.310, 69.170, 3956.3, 5.540, 77.710, 69.170, 3956.2, 5.540,
52.310, 69.170, 168.5} * 10-3;
c = 299 792 458;
charge = 1 * 10-12;
Np = charge / (1.6 * 10-19);
mur = 1;
re = 2.818 * 10-15;
E0 = 0.51 * 106;
phi = 0;
r0 = 0;
```

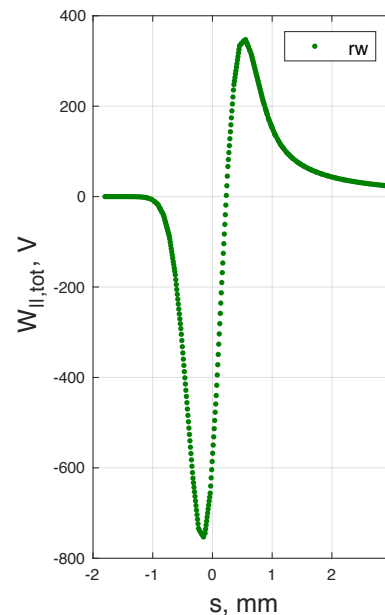
Mathematica Script

- The rw wakefield is generated in Mathematica using the analytical approach developed by K. Bane & M. Sands or A. Piwinski.

*K. Bane & M. Sands, SLAC-PUB-95-7074
A. Piwinski, DESY Report 72/72, 1972*

$$W_{||,rw}(s) = 0.8 \times \frac{r_e m c^2 N_e}{2b \sqrt{2\mu_r Z_0 \sigma_{con}}} \left| \frac{s}{\bar{\sigma}_s} \right|^{3/2} e^{-s^2/4\bar{\sigma}_s^2} \times \left[I_{1/4} \left(\frac{s^2}{4\bar{\sigma}_s^2} \right) - I_{-3/4} \left(\frac{s^2}{4\bar{\sigma}_s^2} \right) - \text{sgn}(s) I_{-1/4} \left(\frac{s^2}{4\bar{\sigma}_s^2} \right) + \text{sgn}(s) I_{3/4} \left(\frac{s^2}{4\bar{\sigma}_s^2} \right) \right]$$

Arcs + LS +SS



Short & Long Straights Sec.

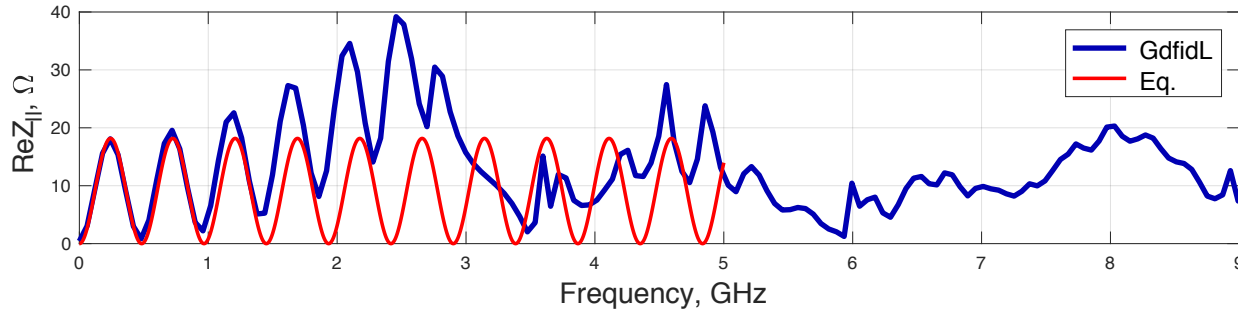
<input type="checkbox"/> Wrw_03.dat	<input checked="" type="checkbox"/> Wrw_02
<input checked="" type="checkbox"/> Wrw_03.nb	<input type="checkbox"/> Wrw_02.dat
<input type="checkbox"/> Wrw_05.dat	<input checked="" type="checkbox"/> Wrw_04
<input checked="" type="checkbox"/> Wrw_05.nb	<input type="checkbox"/> Wrw_04.dat
<input type="checkbox"/> Wrw_07.dat	<input checked="" type="checkbox"/> Wrw_10
<input checked="" type="checkbox"/> Wrw_07.nb	<input type="checkbox"/> Wrw_10.dat
<input type="checkbox"/> Wrw_11.dat	<input type="checkbox"/> Wrw_12.dat
<input checked="" type="checkbox"/> Wrw_11.nb	<input checked="" type="checkbox"/> Wrw_12.nb
<input type="checkbox"/> Wrw_17.dat	<input type="checkbox"/> Wrw_16.dat
<input checked="" type="checkbox"/> Wrw_17.nb	<input checked="" type="checkbox"/> Wrw_16.nb
<input type="checkbox"/> Wrw_19.dat	<input type="checkbox"/> Wrw_22.dat
<input checked="" type="checkbox"/> Wrw_19.nb	<input checked="" type="checkbox"/> Wrw_22.nb
<input type="checkbox"/> Wrw_21.dat	<input type="checkbox"/> Wrw_24.dat
<input checked="" type="checkbox"/> Wrw_21.nb	<input checked="" type="checkbox"/> Wrw_24.nb
<input type="checkbox"/> Wrw_23.dat	<input type="checkbox"/> Wrw_30.dat
<input checked="" type="checkbox"/> Wrw_23.nb	<input checked="" type="checkbox"/> Wrw_30.nb
<input checked="" type="checkbox"/> Wrw_191315252729	<input type="checkbox"/> Wrw_081828.dat
<input type="checkbox"/> Wrw_191315252729.dat	<input checked="" type="checkbox"/> Wrw_081828.nb
<input type="checkbox"/> Wrw_SSS.dat	<input checked="" type="checkbox"/> Wrw_06142026
	<input type="checkbox"/> Wrw_06142026.dat
	<input type="checkbox"/> Wrw_LSS.dat

Geometric Impedance

Stripline Kicker

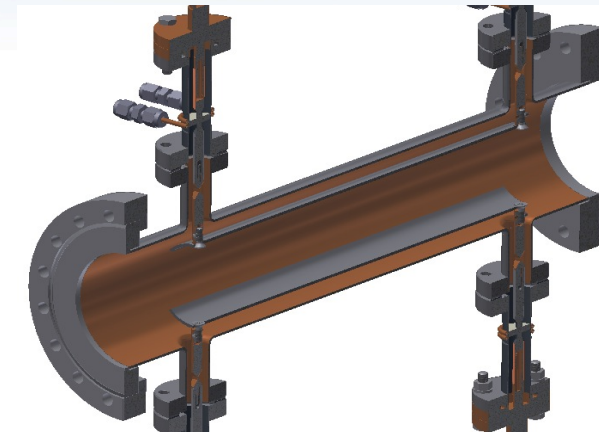
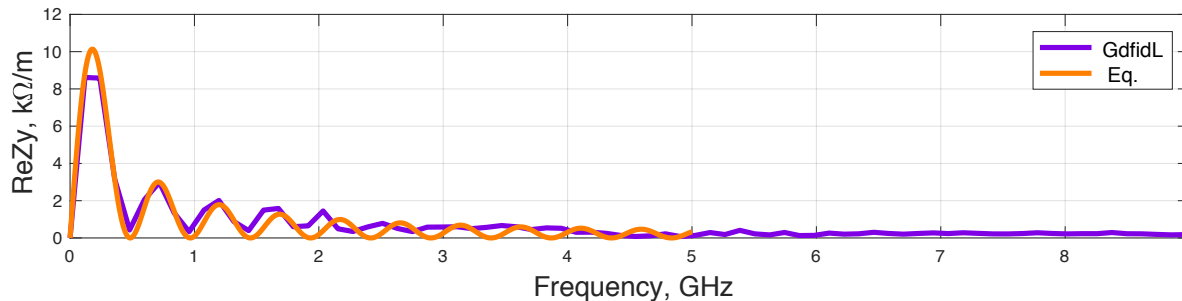
- Longitudinal Impedance $g_{\parallel} = 0.77, Z_{ch,\parallel} = 30.4\Omega$

$$Z_{\parallel}(k) = g_{\parallel}^2 Z_{ch,\parallel} [\sin^2(kL) + j \sin(kL) \cos(kL)]$$

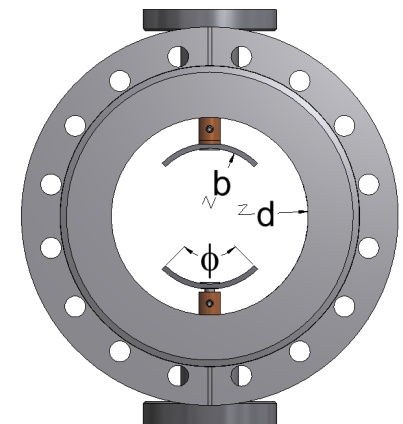


- Transverse Impedance $g_{\perp} = 1.07, Z_{ch,\perp} = 25\Omega$

$$Z_{\perp}(k) = (g_{\perp}^2 Z_{ch,\perp} / kb^2) [\sin^2(kL) + j \sin(kL) \cos(kL)]$$



$b=25.2\text{mm}, t=2\text{mm}, 90^\circ,$
 $d=39.69\text{mm}, L=310\text{mm}$



Z_{ch} and g can be found analytically or numerically with 2D POISSON Code

D.A. Goldberg and G.R. Lambertson, "Dynamic Devices: A Primer on Pickups and Kickers," LBL-31664, 1991

A. Blednykh, W. Cheng, S. Krinsky, "Stripline Beam Impedance" NAPAC13

Impedance Budget

Longitudinal $W_{||}$ for $\sigma_s=0.3\text{mm}$

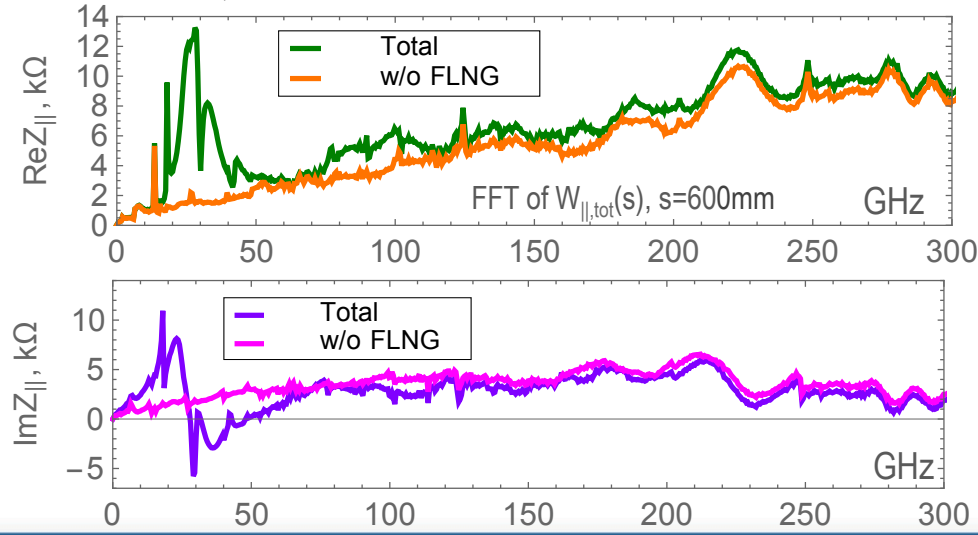
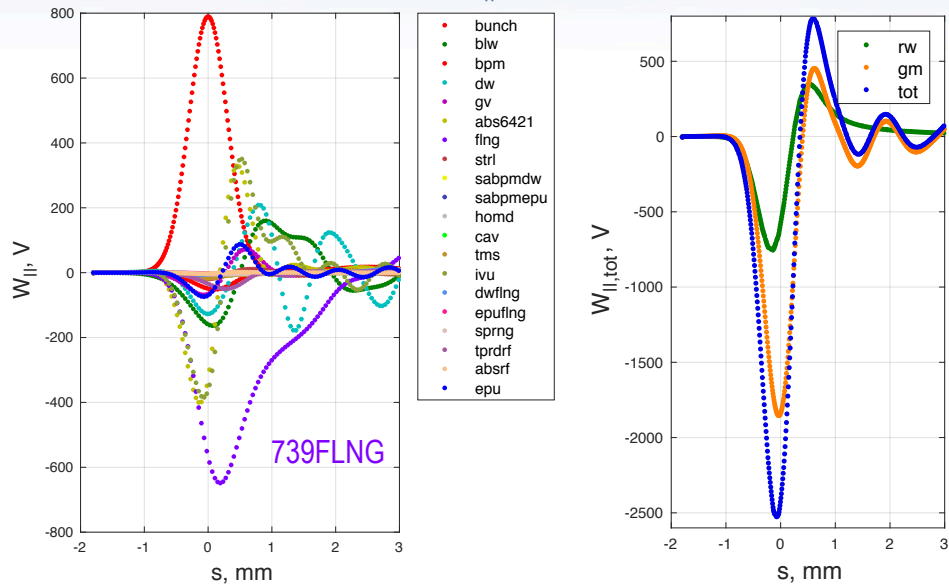
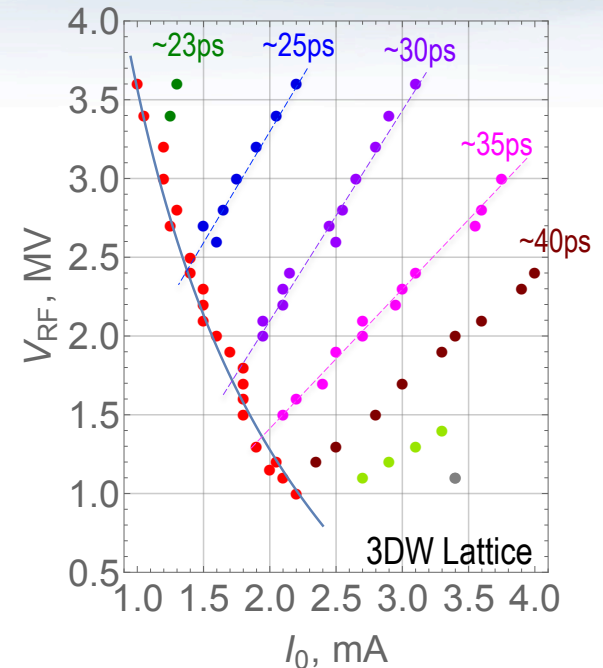
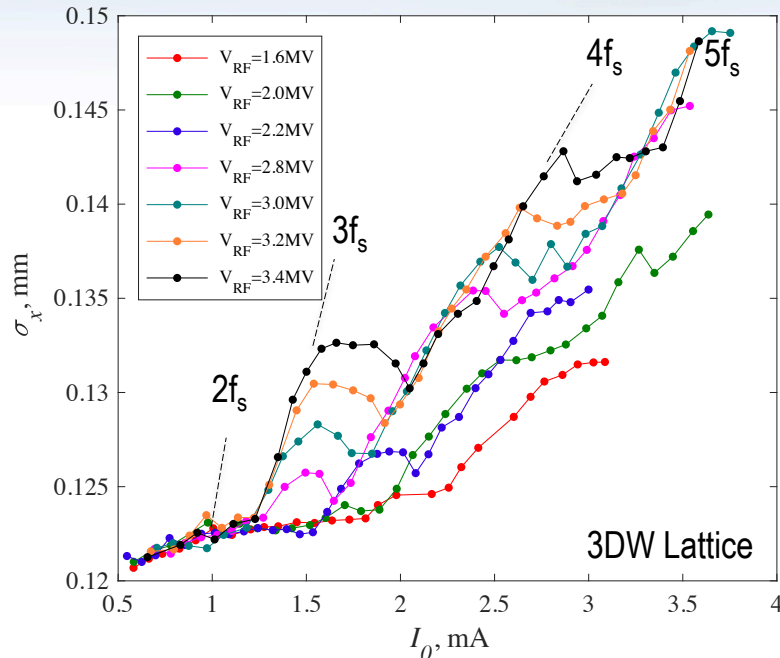


Table: List of the NSLS-II vacuum components

		Number of components
Bellows	BLW	218
Large Aperture BPM	LABPM	237
Small Aperture BPM (11.5mm x 60mm)	SABPMDW	10
Small Aperture BPM (8mm x 55mm)	SABPMepu	3
Damping Wiggler Chamber (11.5mm x 60mm)	DW	3
Elliptically Polarized Undulator Chamber (11.5mm x 60mm)	EPU1	2
Elliptically Polarized Undulator Chamber (8mm x 55mm)	EPU2	2
Gate Valve (Standard)	GV	61
Flange Absorber (21mm x 64mm)	FABS	67
Flange Absorber S4 (21mm x 64mm)	FABSS4	39
Flange Absorber Rest	FABS2	7
Stripline (BBF), L=300mm	SL300	2
Standard RF Sealed Flanges	FLNG	739
EPU RF Sealed Flanges	EPUFLNG	4
DW RF Sealed Flanges	DWFLNG	13
Direct-Current Current Transformer	DCCT	1
Kickers Ti-Coated Ceramics Chambers	CCHM	5
RF HOM Damper	HOMD	2
500 MHz RF Cavity*	CAV	2
RF Tapered Transition	TPRDRF	1
RF Flange Absorber (21mm x 64mm)	FABSRF	1
Stripline (TMS), L=150mm	SL150	2
In-Vacuum Undulator	IVU	9

* The fundamental E_{010} -Mode was subtracted from the GdfidL simulated wakepotential of the RF cavity using the following electrodynamic parameters, $R_{sh,||} = 33375M\Omega$, $Q_0 = 750 \times 10^6$ and $f_r = 502MHz$ and the Broad-Band Resonator (BBR) analytical expression.

Microwave Instability Measurements in NSLS-II

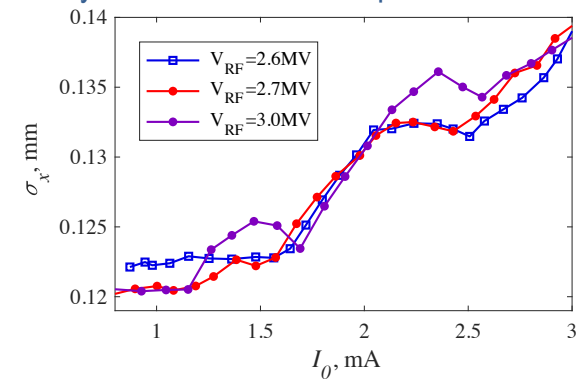


3DW lattice and all other ID's gap open (Aug. 28, 2016). Measurements of the horizontal beam size vs. single bunch current at different RF voltages using SLM Camera. The error bars has been omitted on this plot for better data representing.

- Horizontal beam size σ_x vs sb current I_0 measured at different RF voltages V_{RF} for Bare lattice & 3DW lattice
- Different diagnostic methods: SLM, IVU spectrum at 5th & 7th harmonics, Beam spectra.
- Non-Uniform Intensity related waveform beam pattern

A. Blednykh, B. Bacha, G. Bassi, O. Chubar, M. Rakhitin, V. Smaluk, M. Zhernenkov, Proceedings of IPAC2017, Copenhagen, Denmark

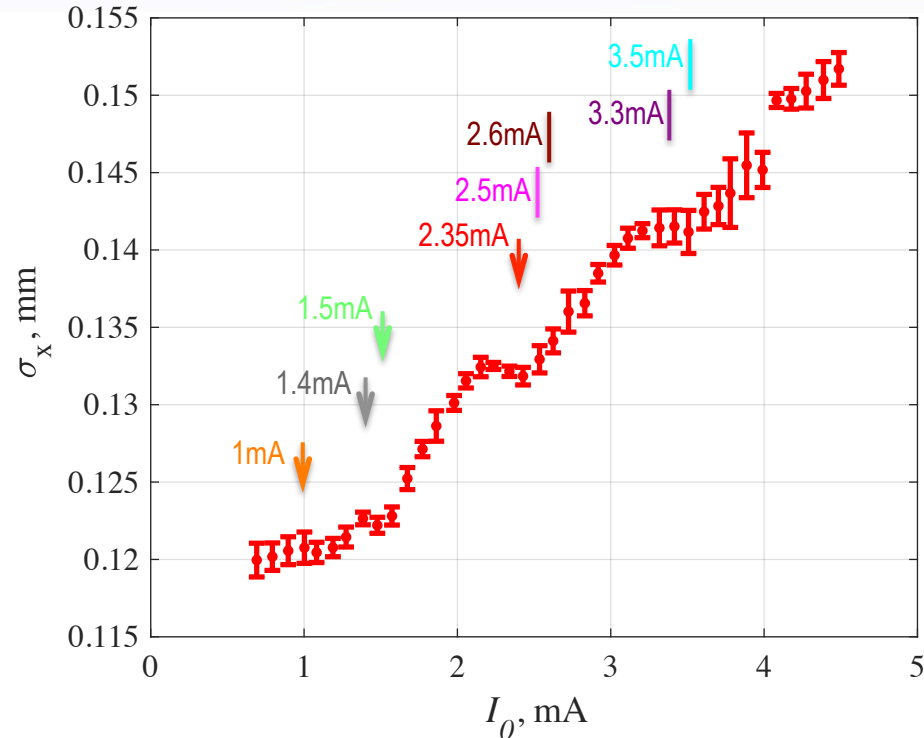
Summary of microwave beam pattern at different V_{RF}



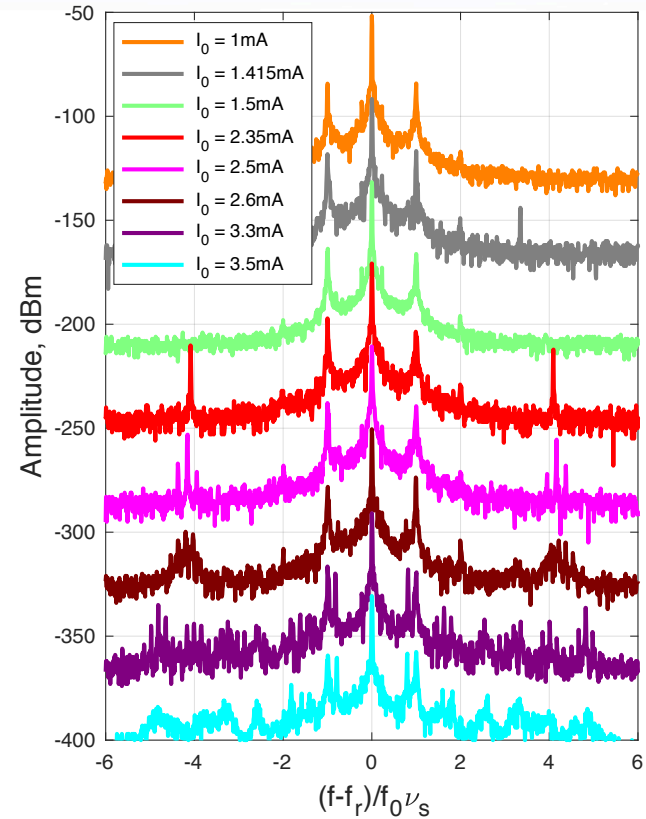
Horizontal beam size measurements from SLM camera vs single bunch current for 3DW lattice

Microwave Beam Pattern and Beam Spectra

3DW Lattice, $V_{RF}=2.7\text{MV}$

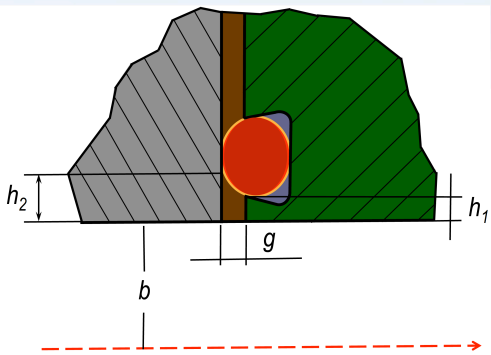


Horizontal beam size vs single-bunch current

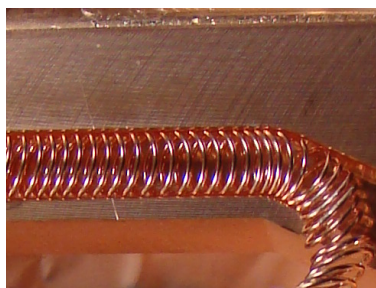


Beam spectra measurements with
ESA 4405B spectrum analyzer

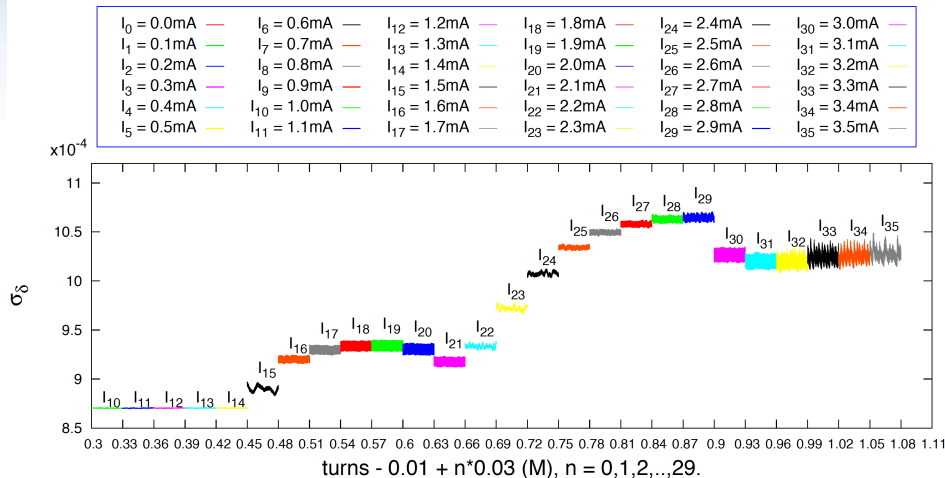
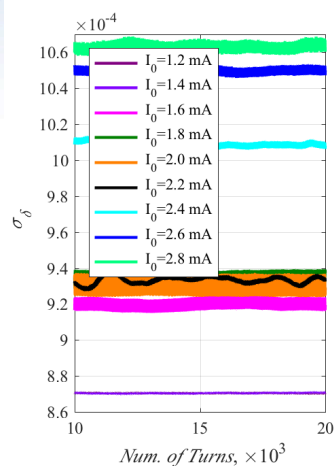
Beam Dynamics Simulations with $W_{\parallel, \text{tot}}(s)$



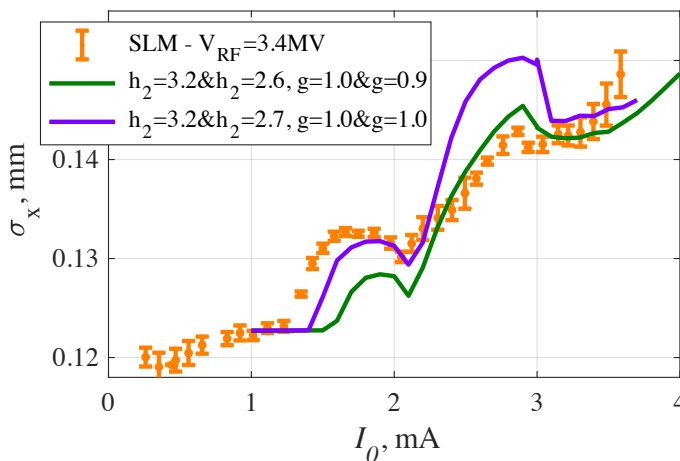
Sketch of the flanges joint with assembled RF contact spring



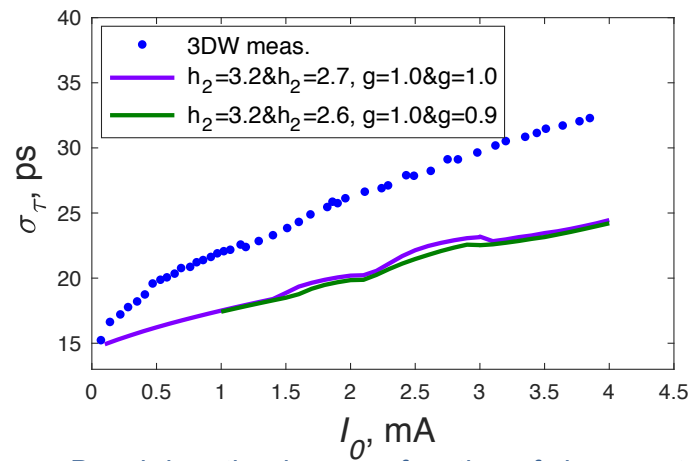
Partial view of the RF contact spring installed in the trapezoidal groove



SPACE code simulations for the 3DW lattice at $V_{RF}=3.4\text{MV}$



Horizontal beam size vs sb current



Bunch lengthening as a function of sb current

- Beam dynamics simulations reproduce microwave beam pattern
- Discrepancy in bunch lengthening simulations needs to be understood

A. Blednykfi, B. Bacha, G. Bassi, W. Cheng, O. Chubar, M. Raĳitin, V. Smaluk, M. Zhernenkov, Y. Chen-Wiegart and L. Wiegart, NLSLS-II TechNote – 239, 2017

Concluding Remarks

- Impedance modeling approach has been discussed.
- Microwave instability thresholds estimated numerically using the calculated impedance/wakefield and compared with measured SLM camera data. The results are in reasonable agreement.
- Discrepancy in bunch lengthening simulations is under investigation. Low frequency contribution?
- Analysis of beam spectra in progress.

Acknowledgments

- BNL/NSLS-II

B. Bacha, G. Bassi, G. Wang, T. Shafiq, V. Smaluk, W. Cheng, S. Kramer, L.-H. Yu, D. Padrazo, E. Zitvogel, A. Derbenev, R. Smith, R. Reiner, O. Chubar, Y. Chen-Wiegart, M. Zhernenkov, M. Rikitin, L. Wiegart, B. Podobedov, A. Fluerasu, C. Hetzel, Y. Li, B. Kosciuk, Y. Hidaka, J. Choi.

- ANL/APS

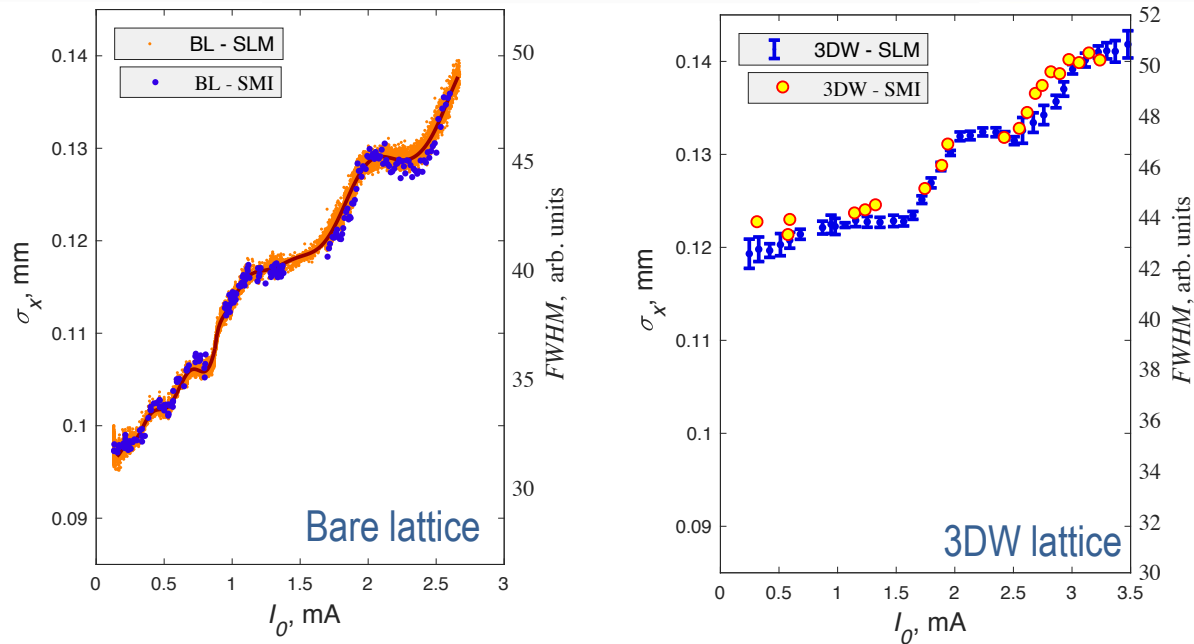
R. Lindberg, B. Stillwell

- SLAC National Accelerator Laboratory

K. Bane, G. Stupakov

Back - Up

Microwave Instability Measurements in NSLS-II

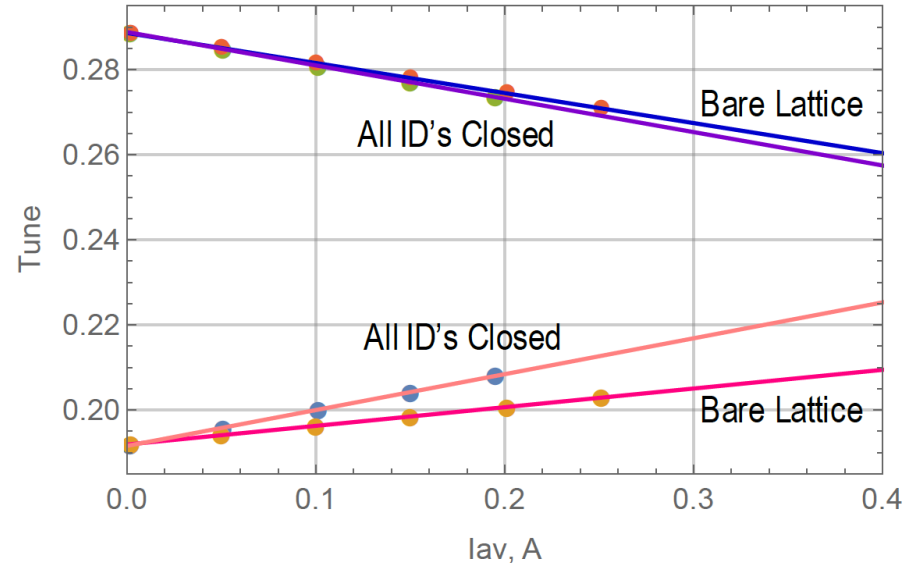


Horizontal beam size (σ_x) measurements from SLM camera and FWHM measured from the IVU spectrum of 7th harmonic at $V_{RF}=2.6\text{MV}$ for the two different lattices.

Tune Shift Dependence On The Average Current

Beamline Shutter Endline Control

Beamline Control	Beamline Control		ID Gap (mm)		
	ID Gap	BMPS	Detail	ID 1	ID 2
2 SIX	Open	Open	EPU57	220.0	
3 HXN	Closed	Open	IVU20	6.63	
4 ISR	Closed	Open	IVU23	10.00	
5 SRX	Closed	Open	IVU21	6.92	
8 ISS	Closed	Open	DW100	15.0	15.0
8BM TES	None	Open			
10 IXS	Closed	Open	IVU22	7.73	
11 CHX	Closed	Open	IVU20	6.64	
11BM CMS	Inserted	Open	3PW	0.0	
12 SMI	Open	Open	IVU23	40.00	
16 LIX	Closed	Open	IVU23	5.91	
17 AMX/FMX	Closed	Open	IVU21	6.75	7.00
17BM XFP	Inserted	Open	3PW	0.0	
18 FXI	Closed	Open	DW100	15.0	15.0
19 NYX	Open	Closed	IVU18	20.30	
21 ESM	Closed	Open	EPU57	36.3	
23 CSX	Closed	Open	EPU49	20.0	30.8
28 XPD	Closed	Open	DW100	15.0	15.0



Horizontal and vertical betatron tune shifts vs. average current

Tune Slope

- Bare Lattice: $\frac{dv_x}{dI_{av}} = 0.044$, $\frac{dv_y}{dI_{av}} = 0.071$
- All ID's closed : $\frac{dv_x}{dI_{av}} = 0.083$, $\frac{dv_y}{dI_{av}} = 0.079$

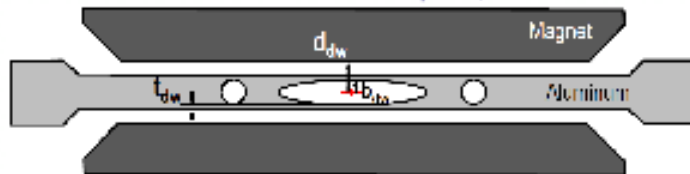
Contributors: Banding Magnets, Multipoles Magnets, ID's

Low – Frequency Quadrupole Impedance Of Undulators and Wigglers

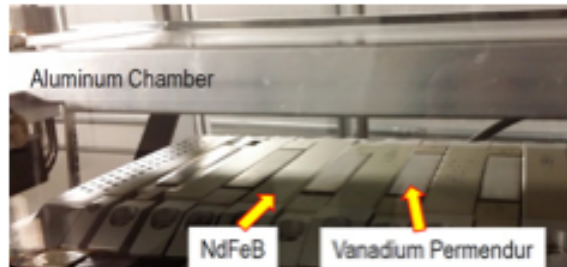
A. Blednykh, G. Bassi, Y. Hidaka, V. Smaluk, Brookhaven National Laboratory, Upton, NY 11973, USA

G. Stupakov, SLAC National Accelerator Laboratory, Menlo Park, CA 94025, USA

Phys. Rev. Accel. Beams **19**, 104401 (2016)



Damping wiggler chamber cross-section with magnetic gap closed, $d_{dw} > t_{dw} + b_{dw}$ and $t_{dw} \ll b_{dw}$



Damping wiggler at open position and the aluminum vacuum chamber (side-view)

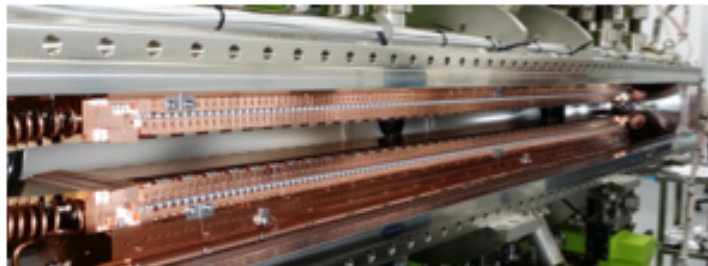
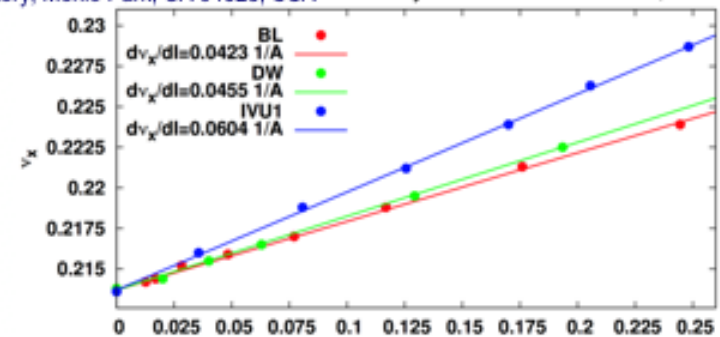
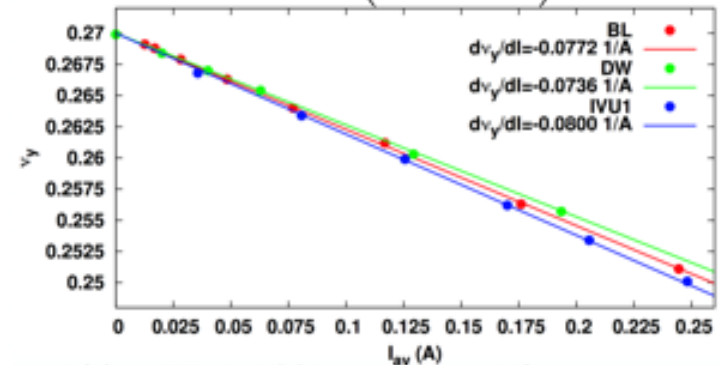


Image of IVU without side cover



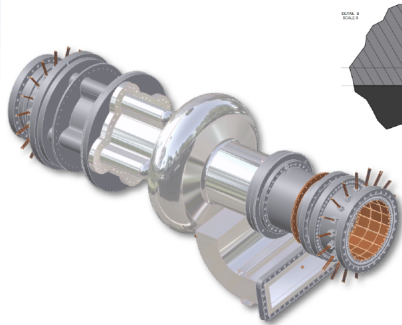
$$Z_{Qx,y}^{IVU}(d) = \pm i \frac{\pi^2}{12c(d-t)^2} \left(1 + 2 \frac{(d-t)^2}{d^2} f(\eta) \right) I_{av} \text{ (A)}$$

$$Z_{Qx,y}^{DW}(d) = \pm i \frac{\pi^2}{12cb^2} \left(1 + \frac{2b^2}{d^2} f(\eta) \right)$$

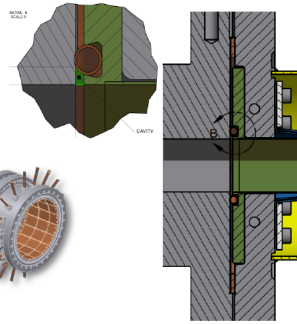


Horizontal (a) and Vertical (b) betatron tune shifts versus average current for lattices with local $\beta_{\perp} = 21m$.

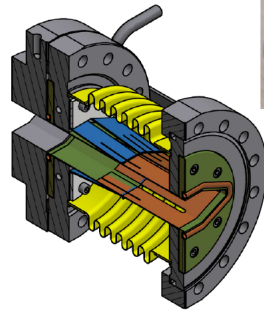
Vacuum Components



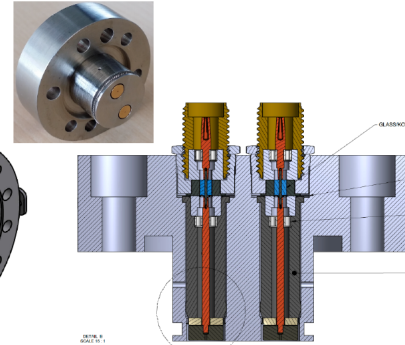
500 MHz RF Cavity



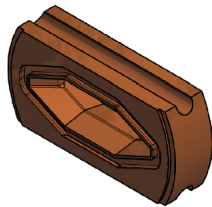
RF Shielded Flanges



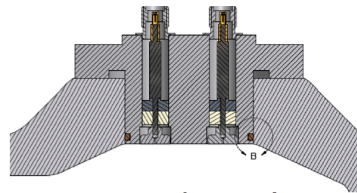
RF Shielded Bellows



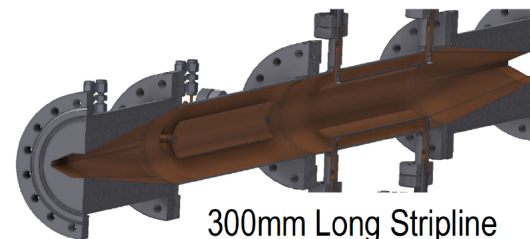
Small Aperture BPM



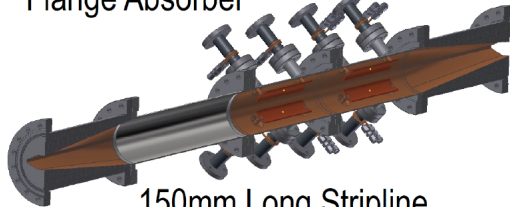
Flange Absorber



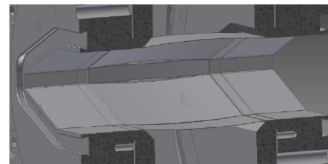
Large Aperture BPM



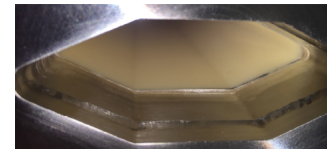
300mm Long Stripline



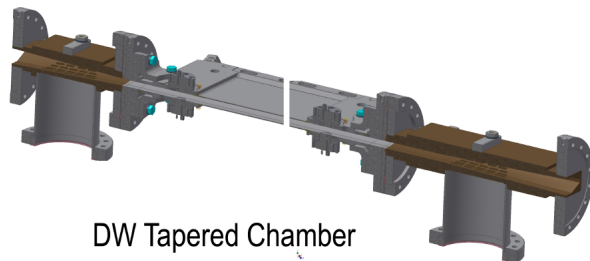
150mm Long Stripline



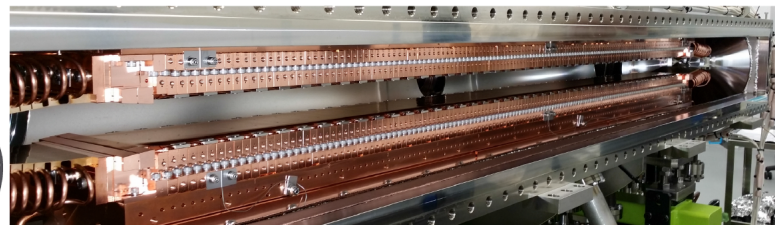
RF Shielded Gate Valve



Ceramic Chambers



DW Tapered Chamber

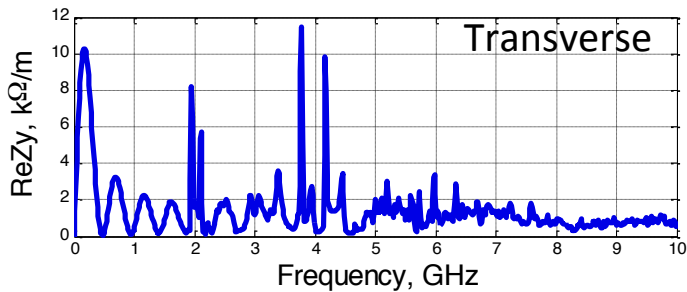
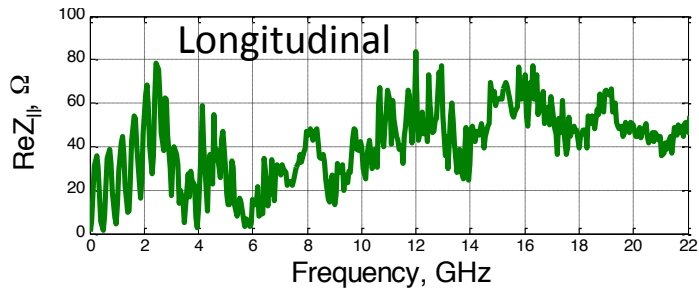
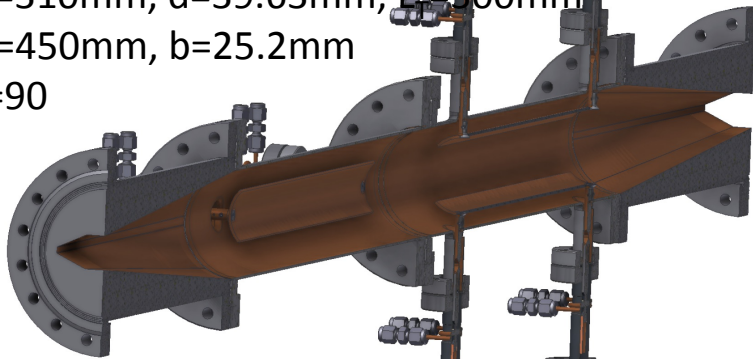


In-Vacuum Undulator

Diagnostic Straight Section (Cell16)

Bunch-by-Bunch Transverse Feedback System

$L_e=310\text{mm}$, $d=39.63\text{mm}$, $L_p=300\text{mm}$
 $L_p=450\text{mm}$, $b=25.2\text{mm}$
 $\phi=90$



Tune Measurements System

